Available online at www.sciencedirect.com
SCIENCE DIRECT®
International Journal of Rock Mechanics & Mining Sciences 42 (2005) 639–651
International Journal of Rock Mechanics and Mining Sciences
www.elsevier.com/locate/ijrmms

Modelling the FEBEX THM experiment using a state surface approach

T.S. Nguyen[a,*], A.P.S. Selvadurai[b], G. Armand[b,1]

[a]Canadian Nuclear Safety Commission, 280 Slater, Ottawa, Canada, K1P 5S9
[b]McGill University, Montreal, Canada, H3A 2T5

Accepted 2 March 2005
Available online 26 April 2005

Abstract

Buffer materials being considered as engineered barriers in nuclear fuel waste (NFW) disposal systems possess a pronounced nonlinear behaviour in the unsaturated state. In order to simulate such non-linear responses,the authors adopted an incrementally nonlinear poro-elastic approach where the coefficients of the governing equations are assumed to be functions of suction and the void ratio. These functions are in turn developed from a state-surface equation obtained from suction-controlled oedometric tests. In this paper we show the derivation of the governing equations of the poro-elastic model. A finite element computer code, FRACON, was developed by the authors to numerically solve the above equations. We first use the code to simulate laboratory tests to characterize the swelling properties of a typical bentonite. That same bentonite was used in the FEBEX in-situ heater experiment, conducted at the Grimsel site, Switzerland. The FRACON code was also used to perform blind predictions of the FEBEX heater experiment. It is shown that the model correctly predicts drying of the bentonite near the heaters and re-saturation near the rock interface. The evolution of temperature and the heater thermal output were also reasonably well predicted by the model. The trends in the total stresses developed in the bentonite were correctly predicted; the absolute values however were underestimated probably due to the omission of pore pressure build-up in the rock mass.

Keywords: Unsaturated; Bentonite; Model

1. Introduction

Concepts for deep geological disposal of nuclear fuel waste (NFW) that are being studied in Canada and other countries rely on the host rock, on clay materials (buffer and backfill) and on the waste containers as barriers against contaminant migration to the biosphere. The focus of this paper is on the modelling of the buffer material. The radiogenic heat released from the waste container results in elevated temperatures around the container, creating a thermal gradient with the attendant thermal stresses and strains in the partially saturated buffer. This thermal gradient also causes moisture movement in the buffer through a diffusive process, resulting in drying near the canister and re-wetting near the buffer-rock interface. The buffer responds mechanically to that change in water content by either shrinking or swelling. These thermo-hydro-mechanical (THM) processes are strongly coupled, and highly nonlinear. In the last decade, much effort has been provided in the laboratory and in-situ experimentation in conjunction with the development of mathematical models to simulate the THM behaviour of unsaturated buffer material. The Kamaishi Mine project in Japan is one such example [1–5] of a comprehensive experimental and theoretical research program involving international cooperation. The FEBEX project [6] is another research project which was recently completed. The FEBEX in-situ experiment was performed in

*Corresponding author. Tel.: +1 613 996 1436; fax: +1 613 996 2049.
E-mail address: nguyens@cnsc-ccsn.gc.ca (T.S. Nguyen).
[1]Currently with ANDRA, Bure, France.

1365-1609/$ - see front matter © 2005 Elsevier Ltd. All rights reserved.
doi:10.1016/j.ijrmms.2005.03.005

one section of a horizontal tunnel in a granitic rock formation at Grimsel, Switzerland. The tunnel section was provided with two heaters and filled with prefabricated bentonite blocks that were placed around the heaters. The THM response of both the bentonite and the surrounding rock was monitored during the experiment. The authors belonged to the Canadian team, among many international teams, participating in the prediction of the FEBEX experiment within the international DECOVALEX III Project. The present paper describes the development of our mathematical model to simulate the THM behaviour of the bentonite used in the in-situ heater experiment and summarizes the results of the model predictions of the THM response of the bentonite during the FEBEX in-situ experiment.

2. A brief overview of THM models for unsaturated clays

For completeness, we provide here a brief review of models that have been proposed for examining the THM behaviour of unsaturated clays. This review is by no means comprehensive; a more thorough discussion could be found in Rutqvist et al. [4].

Partially saturated clay materials are basically multiphase materials, consisting of the solid skeleton with a mixture of air and water flowing through the pore space. The air can be dissolved in the liquid water, or be present in a gaseous state; the water could also be present in a gaseous or liquid state. In order to develop mathematical models for the coupled THM behaviour of such a system, one has to satisfy conservation laws for mass, energy and momentum in addition to a number of assumptions pertaining to constitutive relations. This approach results in the following four governing equations for: mass balance for the air phase, mass balance for the water phase, energy balance and momentum balance [7–10]. The mechanical behaviour of partially saturated soils depends on at least two independent stress state variables, such as the net stress and suction. A state space surface approach as proposed by certain authors [11,12] or a recent elasto-plastic approach proposed by Alonso et al. [13] could be used to formulate constitutive relationships governing net stress, suction and strain.

Recently, researchers involved in the prediction of the Kamaishi Mine Experiment have assumed a constant and small gas pressure (equal to atmospheric pressure) in their models, thereby reducing the governing equations to three: mass balance for the water phase, energy balance and momentum balance [3–5]. The primary unknowns of the equations are temperature, displacement and the capillary pressure. This simplification seems to be justified from the reasonable predictions obtained by these researchers and independently by other investigators [14], when maximum temperatures are not significantly higher than 100 °C, which indeed is the design maximum temperature for HLW disposal in granitic rocks. Furthermore, one single state variable, such as the modified effective stress proposed by Bishop and Blight [15] or by Biot [16] in his classical work was adopted by the investigators working on developing the predictions of the Kamaishi Mine Experiment. Generally, it is recognized that the adoption of one single state variable has shortcomings [17] since non-recoverable strain due to wetting-drying could not be simulated. However, for the highly compacted bentonite that is maintained in a constrained condition, such as that used in the Kamaishi Mine in-situ heater experiment and similar systems intended for HLW disposal, this approach could prove to be sufficient.

The model we present in this paper is based on the classical Biot's poro-elastic approach, extended to partially saturated materials. A state surface equation as experimentally derived from suction controlled oedometric tests was used to express the constants of poro-elasticity as functions of the void ratio and the applied load. The equations of poro-elasticity were expressed in an incremental form to accommodate the pronounced nonlinearity associated with this behaviour. The model was first used to simulate laboratory experiments on the FEBEX bentonite , then for the prediction of the in-situ FEBEX experiment.

3. Governing equations of the model

The governing equations of the mathematical model developed by the authors are derived from energy balance, mass balance and momentum balance considerations.

3.1. Energy balance

Assuming thermal equilibrium between the phases and heat conduction as the dominant mechanism of heat transfer, the energy balance equation reduces to the following (for justifications of these assumptions, see e.g. [18]):

$$\frac{\partial}{\partial x_i}\left(\kappa_{ij}\frac{\partial T}{\partial x_j}\right)+q=\rho C\frac{\partial T}{\partial t}, \tag{1}$$

with T, the temperature of the medium (°C), κ_{ij} the thermal conductivity tensor (W/m/C), ρ the density of the bulk medium (kg/m^3), C the specific heat of the medium (J/kg/C) and q the heat source (W/m^3).

3.2. Momentum balance

Neglecting inertial effects, the momentum balance equation reduces to the equation of equilibrium of the

porous medium:

$$\frac{\partial \sigma_{ij}}{\partial x_j} + F_i = 0, \tag{2}$$

where σ_{ij} is the total stress and F_i is the body force.

Within Biot's theoretical framework, the constitutive equation for poroelasticity was extended to include thermal effects and partial saturation and can be written in incremental form as follows (see e.g. [4]):

$$\begin{aligned} \mathrm{d}\sigma_{ij} &= 2G\,\mathrm{d}e_{ij} + \delta_{ij}\lambda\,\mathrm{d}e_{kk} \\ &\quad + \delta_{ij}(\lambda\,\mathrm{d}e_{kk} - \beta K_{\mathrm{D}}\,\mathrm{d}T) + \delta_{ij}\alpha S\,\mathrm{d}p, \end{aligned} \tag{3}$$

where G, λ are the Lame's constants; α is the pseudo-Biot's coefficient; S is the degree of saturation; p is the liquid pressure; and e_{ij} is the small strain tensor defined by

$$e_{ij} = \frac{1}{2}\left(\frac{\partial u_i}{\partial x_j} + \frac{\partial u_j}{\partial x_i}\right). \tag{4}$$

The effective stress increment in Eq. (3) would be given by

$$\mathrm{d}\sigma'_{ij} = 2G\,\mathrm{d}e_{ij} + \delta_{ij}\lambda\,\mathrm{d}e_{kk} + \delta_{ij}(\lambda\,\mathrm{d}e_{kk} - \beta K_{\mathrm{D}}\,\mathrm{d}T). \tag{5}$$

Substitution of Eq. (4) into Eq. (3) yields:

$$\begin{aligned} &G\frac{\partial^2 \mathrm{d}u_i}{\partial x_j \partial x_j} + (G+\lambda)\frac{\partial^2 \mathrm{d}u_j}{\partial x_i \partial x_j} + \alpha S\frac{\partial\,\mathrm{d}p}{\partial x_i} \\ &\quad - \beta K_{\mathrm{D}}\frac{\partial\,\mathrm{d}T}{\partial x_i} + \mathrm{d}F_i = 0, \end{aligned} \tag{6}$$

where K_{D} the bulk modulus is given by

$$K_{\mathrm{D}} = \lambda + \frac{2G}{3} = \frac{E}{3(1-2\upsilon)}. \tag{7}$$

The final equation of momentum balance (6) is written in incremental form; to take into account the nonlinear behaviour, the poro-elastic coefficients of the equation are expressed as functions of suction and net stress by adopting the concept of a state surface equation [11,12]. This equation relates the void ratio to the applied net stress and the suction. Based on results of oedometric tests, Lloret and Alonso [19] proposed the following state surface equation:

$$e = A + B\ln(-\sigma''_m) + C\ln(s+p_{\mathrm{a}}) + D\ln(-\sigma''_m)\ln(s+p_{\mathrm{a}}), \tag{8}$$

where e is the void ratio; p_{a} is atmospheric pressure; A, B, C and D are empirical constants; $\sigma''_m = (\sigma_{kk}/3) - p_{\mathrm{g}}$ is the mean net stress and $s = p - p_{\mathrm{g}}$ is the suction, where p_{g} is the gas pressure. Since we assume that the gas pressure is small and constant:

$$\mathrm{d}\sigma_m = \mathrm{d}\sigma''_m. \tag{9}$$

The increment of the void ratio can then be expressed as

$$\mathrm{d}e = \frac{\partial e}{\partial \sigma''_m}\,\mathrm{d}\sigma_m + \frac{\partial e}{\partial p}\,\mathrm{d}s = \frac{\partial e}{\partial \sigma''_m}\,\mathrm{d}\sigma_m + \frac{\partial e}{\partial p}\,\mathrm{d}p. \tag{10}$$

From Eq. (3), in the isothermal case, the increment of the mean total stress is given by

$$\mathrm{d}\sigma_m = K_{\mathrm{D}}\,\mathrm{d}e_v + \alpha S\,\mathrm{d}s \tag{11}$$

with $\mathrm{d}e_v = \mathrm{d}e_{kk}$, the increment of the volumetric strain.

The volume variation is given by simple phase relationships:

$$\mathrm{d}e_v = \frac{\mathrm{d}e}{1+e}. \tag{12}$$

Substituting the right-hand side of Eq. (10) into Eq. (12), one has:

$$\mathrm{d}e_v = \frac{1}{1+e}\left[\frac{\partial e}{\partial \sigma''_m}\,\mathrm{d}\sigma''_m + \frac{\partial e}{\partial s}\,\mathrm{d}s\right]. \tag{13}$$

Comparing Eqs. (10) and (12), one obtains:

$$\frac{1}{K_{\mathrm{D}}} = \left(\frac{1}{1+e}\right)\frac{\partial e}{\partial \sigma''_m}, \tag{14}$$

$$\frac{-\alpha S}{K_{\mathrm{D}}} = (1+e)\frac{\partial e}{\partial s}. \tag{15}$$

Performing differentiation of the state surface equation (8), one obtains:

$$K_{\mathrm{D}} = \frac{(1+e)\sigma''_m}{B + D\ln(s+p_{\mathrm{a}})} \tag{16}$$

and

$$\alpha = -\frac{1}{S}\frac{\sigma''_m}{B + D\ln(s+p_{\mathrm{a}})}\frac{C + D\ln(-\sigma''_m)}{s+p_{\mathrm{a}}}. \tag{17}$$

From elementary phase relationships in soil mechanics, $S = (G_{\mathrm{s}}/e)w$, where w is the water content and G_{s} is the specific weight of the solids.

For suction varying between 2.0 and 385.0 MPa, empirical equations relating water content and suction could usually be determined for bentonite, independently of the dry density. For example, the suction characteristics of the bentonite used in the FEBEX in-situ heater experiment could be represented by the following empirical function [20]:

$$w = 36.1 - 12.0\log s, \tag{18}$$

where log is the decimal logarithmic function (base 10), w is in %, and s is in MPa.

From Eq. (7), one can show:

$$\sigma''_m = -\exp\left(\frac{e - A - C\ln(s+p_{\mathrm{a}})}{B + D\ln(s+p_{\mathrm{a}})}\right). \tag{19}$$

Substituting Eq. (19) into Eqs. (16) and (17), K_D and α are expressed entirely as functions of s and e.

3.3. Water mass balance

The equation of mass balance of the pore water, neglecting vapour storage is

$$-\frac{\partial}{\partial x_i}(Q_{li}+Q_{vi}) = \frac{\partial}{\partial t}(nS\rho_f) = nS\frac{\partial \rho_f}{\partial t} + n\rho_f\frac{\partial S}{\partial t} + S\rho_f\frac{\partial n}{\partial t}, \quad (20)$$

where Q_{li} and Q_{vi} (kg/(m^{2}s) are respectively the liquid water mass flux and the water vapour mass flux relative to the solid; n is porosity; S is the degree of saturation and ρ_f (kg/m^3)is the density of water. For liquid water flux, we use an extended form of Darcy's law applicable to a partially saturated medium (see e.g. [21]):

$$Q_{li} = -\rho_f\frac{k_{ij}}{\mu}k_r\left(\frac{\partial p}{\partial xj}+\rho_f g_i\right), \quad (21)$$

where k_{ij} is the intrinsic saturated permeability [m^2] and k_r is the relative permeability. The water vapour flux on the other hand is assumed to be driven solely by the thermal gradient:

$$Q_{vi} = -\rho_f D_T\frac{\partial T}{\partial x_i}, \quad (22)$$

where D_T (m^2/s/°C) is the thermal vapour diffusivity coefficient.

We now expand the right-hand side of Eq. (20). The constitutive relationship for the pore fluid could be written as

$$d\rho_f = \rho_f\left(\frac{dp}{K_f}+\beta_f\,dT\right) \quad (23)$$

with K_f = bulk modulus of fluid and β_f = Coefficient of volume thermal expansion of the fluid. Then:

$$nS\frac{\partial \rho_f}{\partial t} = -nS\rho_f\left(\frac{1}{K_f}\frac{\partial p}{\partial t}+\beta_f\frac{\partial T}{\partial t}\right). \quad (24)$$

Usually S is experimentally determined as a function of suction:

$$\frac{\partial S}{\partial t} \cong \left(\frac{dS}{ds}\right)\frac{\partial s}{\partial t} = \left(\frac{dS}{dp}\right)\frac{\partial p}{\partial t}. \quad (25)$$

In Eq. (25) and in the following equations, we assume small and constant gas pressure, and with the convention of tension-positive for the liquid pressure, so that

$$ds = dp. \quad (26)$$

In addition to suction, the degree of saturation S depends also on the degree of compaction. Consequently: $S = S(p,n)$. On the other hand, it is often experimentally found that the water content could be expressed as a sole function of suction [19]: $w = w(s)$. Since $S = G_s w/e = (G_s w/n)(1-n)$, we obtain:

$$\frac{dS}{dp} = \frac{G_s(1-n)}{n}\frac{dw}{dp} - \frac{G_s w}{n^2}\frac{dn}{dp}. \quad (27)$$

We now follow Bishop's [22] procedure to express the increment of porosity dn due to change in stress $d\sigma_{ij}$ and temperature dT. The increment of total stress can in turn be represented in terms of two components: an increment in the average fluid pressure (mixture of gas and liquid):

$$dP = S\,dp + (1-S)\,dp_g = S\,dp \quad (28)$$

and an increment in the effective stress $d\sigma'_{ij}$.

The change in volume of the solid due to $S\,dp$ is

$$dV_s = (1-n)V\frac{S\,dp}{K_s}$$

The total volume change due to $S\,dp$ is

$$dV = V\frac{S\,dp}{K_s},$$

The changes in volumes due to $d\sigma'_{ij}$ are:

$$dV_s = \frac{V\,d\sigma'_{kk}}{3K_s},$$

$$dV = \frac{V\,d\sigma'_{kk}}{3K_D}.$$

The changes in volume due to dT are:

$$dV_s = (1-n)V\beta_s\,dT,$$

$$dV = V\beta\,dT.$$

We have:

$$dn = \frac{\sum dV - \sum dV_s}{V},$$

$$dn = nS\frac{dp}{K_s} + \left(\frac{1}{K_D}-\frac{1}{K_s}\right)\frac{d\sigma'_{kk}}{3} + (\beta-(1-n)\beta_s)\,dT. \quad (29)$$

Since:

$$d\sigma'_{kk} = 3K_D\left(de_{kk} - \frac{S\,dp}{K_s} - \beta\,dT\right),$$

with some re-arranging, Eq. (28) becomes:

$$dn = (n-\alpha)S\frac{dp}{K_s} + \alpha\,de_{kk} + ((1-\alpha)\beta-(1-n)\beta_s)\,dT \quad (30)$$

With the use of Eqs. (24)–(27), (29) and (30), the right-hand side of Eq. (20) could be expanded as follows and the final equation for the water mass balance (20) could

be written as follows:

$$\frac{\partial}{\partial x_i}\left(\frac{\rho_f k_{ij} k_r}{\mu}\left(\frac{\partial p}{\partial x_j}+\rho_f g_j\right)\right)-\frac{\partial}{\partial x_i}\left(D_T\frac{\partial T}{\partial x_i}\right)+\rho_f\left[\frac{-nS}{K_f}+G_{sub}(1-n)\frac{dw}{dp}+S\left(S-\frac{G_{sub}w}{n}\right)\times\frac{n-\alpha}{K_s}\right]\frac{\partial p}{\partial t}+\rho_f(S\alpha)\frac{\partial}{\partial t}\left(\frac{\partial u_k}{\partial x_k}\right)+\rho_f S((1-\alpha)\beta-n\beta_f-(1-n)\beta_s)\frac{\partial T}{\partial t}=0. \quad (31)$$

Eqs. (1), (6) and (31) are the governing equations of our mathematical model to simulate the THM behaviour of partially saturated clay material. The equations are solved numerically by the finite element method with the computer code FRACON developed by the authors [18].

4. THM properties of the FEBEX bentonite

The FEBEX bentonite is a Spanish clay considered as the most suitable material for sealing and backfilling of NFW repositories for the Spanish concept [6] for the following reasons: it has a very high content of montmorillonite, low permeability and good retention properties, and is capable of developing large swelling pressures. The characteristics of the FEBEX bentonite are discussed in details in the reports produced by the Spanish research institutions CIEMAT and UPC-DIT [6–20]. In this section, we will only summarize the properties required for our THM model. A large number of such input parameters are required. Certain parameters specifically refer to thermo-physical constants that are applicable to either the solid phase or the fluid phase, and these parameters can often be determined from published data. Other parameters that specifically refer to coupling phenomena require special experiments for their determination. A large number of these parameters have been determined through the course of the experimental research programs at both CIEMAT and UPC-DIT [20] for a pure bentonite to be used in the FEBEX in-situ heater experiment. The values of these parameters as shown below were directly or indirectly determined by CIEMAT and UPC-DIT, unless otherwise noted. Also, it is convenient to categorize these values as follows.

4.1. Physical properties

The physical properties for the compacted bentonite have been determined by using standardized test procedures proposed by ASTM. The properties relevant to the in-situ T-H-M modelling are as follows.

Initial porosity (n) = 0.411 (non-dimensional)

Dry density (ρ_d) = 1600 kg/m^3

Density of the fluid (ρ_f) = 1000 kg/m^3

Specific weight of the solids (G_s) = 2.7

Dynamic viscosity of the pore fluid (μ) = $2.285\times10^{-3}+1.01\times10^{-3}\log(T)$ kg/m/s (from [23])

4.2. Thermal properties

The properties relevant to the THM modelling are as follows:

Coefficient of volumetric thermal expansion of the porous skeleton:

$\beta' = 1.95\times10^{-5}\,^\circ\mathrm{C}^{-1}$

Coefficient of volumetric thermal expansion of the solid material:

$\beta' = 1.95\times10^{-5}\,^\circ\mathrm{C}^{-1}$ (assumed equal to β')

Coefficient of volumetric thermal expansion of the liquid (water):

$\beta_f = 4.684\times10^{-5}+7.486\times10^{-6}\,T\,^\circ\mathrm{C}^{-1}$ (from [23])

Coefficient of thermal vapour diffusivity:

$D_T = 10^{-11}$ m^2/s/°C (Assumed value from experience gained with similar projects [1–5])

Coefficient of the thermal conductivity:

$\kappa = 0.57+0.617978S$ (W/m°C^{-1})

Specific heat of the solid (c_s) = 830 J/kg/°C and specific heat of water (c_f) = 4190 J/kg/°C (from [23])

4.3. Hydraulic properties

The saturated hydraulic conductivity K of the compacted bentonite has been determined using specimens of the FEBEX bentonite that have been compacted to various dry densities ρ_d. The dry densities varied between 1.47 and 1.84 g/cm^3. The empirical relationship derived from these tests takes the form:

$$\log K = -2.96\rho_d - 8.57, \quad (32)$$

ρ_d could in turn be expressed as a function of the porosity from simple phase relationships as

$$\rho_d = G_s(1-n)\rho_w. \quad (33)$$

The permeability k of the poro-elastic material is defined through the conventional relationship:

$$k = \frac{K\mu}{\gamma_w}\ (\mathrm{m}^2), \quad (34)$$

where γ_w is the unit weight of water. In the FRACON code, the porosity of the bentonite is updated at each time step and using Eqs. (32)–(34), the permeability is also updated.

The unsaturated hydraulic conductivity of the bentonite is highly dependent on the degree of saturation S. The experimental results provided by CIEMAT give an

empirical relationship for the "relative permeability" or "relative hydraulic conductivity" of the bentonitic material in terms of the degree of saturation as follows:

$$k_R = \frac{k(S)}{k^+} = \frac{K(S)}{K^*} = S^{\tilde{n}}, \quad (35)$$

where k^* and K^* refer to the respective values at full saturation. These relationships are used in the FRACON computations with $\tilde{n} = 4.64$.

From a knowledge of the "suction-water content relationship" obtained for a porous material, where the moisture variations are allowed to take place at a constant dry density, it is possible to define the "*water retention curve*". With bentonitic materials, this relationship is an essential requirement for the modelling of the hydration of the bentonite. On the basis of experimental data, CIEMAT and UPC have proposed the use of the following modified van Genuchten expression to describe the water retention curve. This basic expression is

$$S = S_0 + (S_{\max} - S_0)\left[1 + \left(\frac{s}{P_0}\right)^{\frac{1}{1-\lambda}}\right]^{-\lambda}\left[1 - \frac{s}{P_0}\right]^{\lambda_s}, \quad (36)$$

where S_0 is the residual degree of saturation, $S_{\max}$ is the maximum degree of saturation, s is the suction (measured in MPa), and P_0 (measured in MPa) and λ, λ_s are material parameters.

All material parameters encountered in the modified van Genuchten expression have been determined by CIEMAT by suction controlled oedometer tests on confined samples with dry densities in the range 1.58 to 1.75 g/cm^3. The parameters of the van Genuchten expressions are highly dependent on the state of compaction, hence on the dry density of the material. Since volumetric deformation could be important during the in-situ T-H-M experiment, we used instead the suction-water content relationship proposed by UPC and CIEMAT:

$$w = 36.1 - 12.0 \log s. \quad (37)$$

According to UPC and CIEMAT, the above relationship does not depend significantly on the degree of compaction of the bentonite.

4.4. Mechanical properties

The two important mechanical properties in our model are the bulk modulus and the pseudo-Biot's coefficient, as detailed in Section 2. Assuming $p_a = 0.1$ MPa, the following values were obtained by best-fitting the state surface Eq. (8) to experimental results obtained by suction-controlled oedometric tests:

$$A = 0.76, \quad B = -0.0552446, \quad C = -0.0406413,$$
$$D = 0.00479977.$$

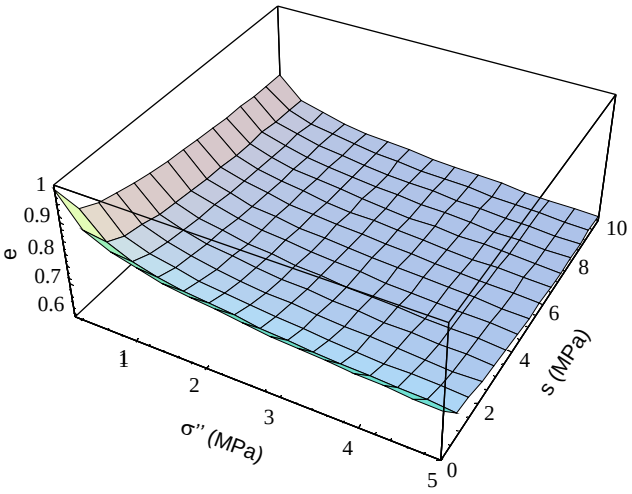

Fig. 1. State surface for the FEBEX bentonite.

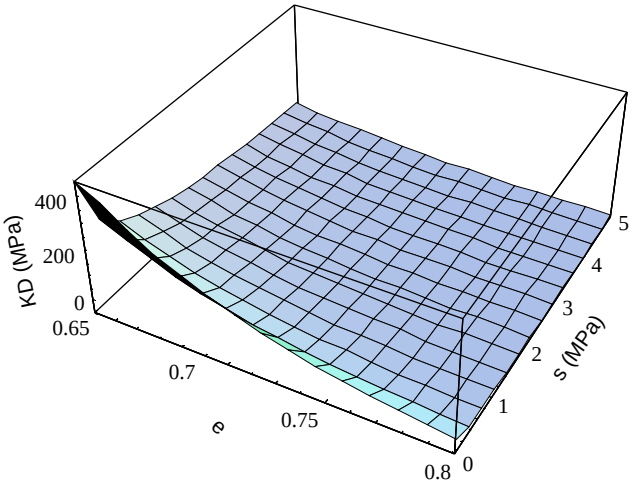

Fig. 2. Bulk modulus of the FEBEX bentonite.

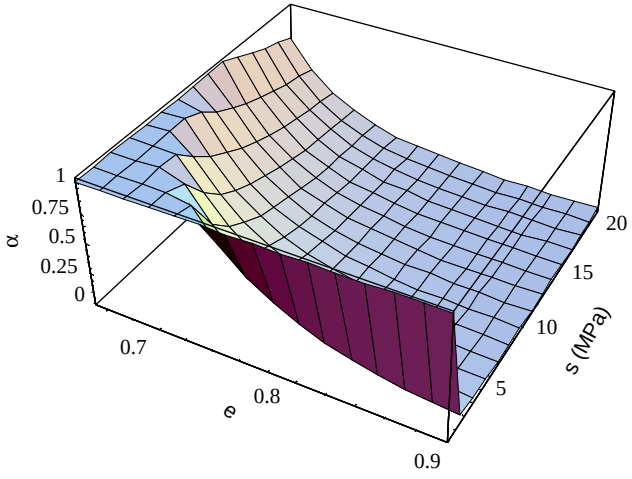

Fig. 3. Pseudo-Biot coefficient.

With the above values, the state space equation (8), the bulk modulus, Eq. (16), and the pseudo Biot coefficient, Eq. (17) are represented as shown in Figs. 1, 2 and 3, respectively. Assuming the Poisson's ratio (v) = 0.30, the values of the Young's modulus to be input to FRACON are calculated according to Eqs. (14) and (17). The Biot's coefficient on the other hand is input to FRACON using Eqs. (15) and (17).

5. Simulation of laboratory experiments on FEBEX bentonite

In order to gain confidence in the THM model implemented in the FRACON finite element code, we have used the code to conduct computational simulations of two types of laboratory experiments. It is important to note that no parametric studies have been conducted, but rather, a direct prediction was carried out using the properties described in Section 4. The sources and justification for the values assumed for these properties were also detailed in Section 4.

5.1. Swelling pressure tests

These tests were performed with oedometers under either strain control or stress control conditions. The oedometer samples were uniaxially compacted bentonite clay contained in oedometer rings 4.93 cm in diameter and 1.20 cm in height. The samples were placed between two porous stones and water was supplied at the base of the cylindrical sample. In this first series of experiments a constant volume condition was achieved by the application of an axial stress to compensate for the volume expansion of the compacted bentonite induced by water uptake. The experimental values of the pressures that are needed to be applied to maintain the zero volume change condition could be best fitted with an empirical relationship of the form:

$$P_S = \exp(5.9\rho_D - 7.9), \tag{38}$$

where P_S is the swelling pressure expressed in MPa and ρ_D is the dry density of the compacted bentonite expressed in g/cm^3.

5.2. Swelling under constant stress

Another set of oedometer tests was conducted to determine the time-dependent development of axial strain in oedometric samples subjected to a constant axial stress. The sample preparation procedure was exactly the same as that described previously for tests involving water uptake under constant volume. Both CIEMAT and UPC-DIT have carried out such tests. The results of interest to the computational modelling exercise concern the time-dependent evolution of swelling strains under constant axial stress.

5.3. Comparison of modelling results with experimental data

The computational modelling involving the FRACON Code utilizes 20-noded brick elements in the discretization of the one-dimensional region. Although the region being modelled is one-dimensional, a three-dimensional representation of the region is employed with suitable adaptation of the boundary conditions that are required to satisfy one-dimensionality. Briefly, the one-dimensional region is modelled by 20-noded elements. The boundary conditions on the displacement, traction and pore pressure variables required to satisfy the one-dimensional behaviour of the element are shown in Fig. 4. (Note that the views shown are for the x–z plane; similar conditions apply for the y–z plane.)

In Fig. 5, the results of the FRACON predictions are compared to the experimental results for the swelling tests under constant volume. The predictions show the evolution of the pressure with time while only the ultimate values are experimentally recorded. The FRACON code predicts the correct experimental trend for the ultimate (steady state) values of the swelling stress: with a higher initial dry density, the swelling stress is higher. The FRACON code slightly underpredicts the ultimate swelling pressure for the lower initial dry density (1.6 g/cm^3) and overpredicts this value by approximately 40% for the higher density (1.7 g/cm^3).

In Fig. 6, the results of the FRACON predictions are compared to the experimental results for the strain development under constant axial load. The trend and magnitude of the strain evolution are reasonably well predicted, with some overestimate of the response time. This shows that the hydraulic characteristics of the

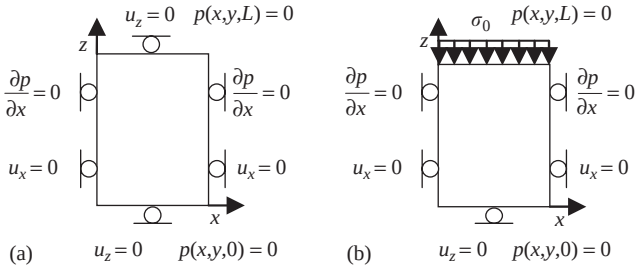

Fig. 4. Schematic view of the one-dimensional problems associated with the moisture uptake and swelling tests. (a) Boundary conditions for the swelling test under constant volume and (b) boundary conditions for the swelling test under constant stress.

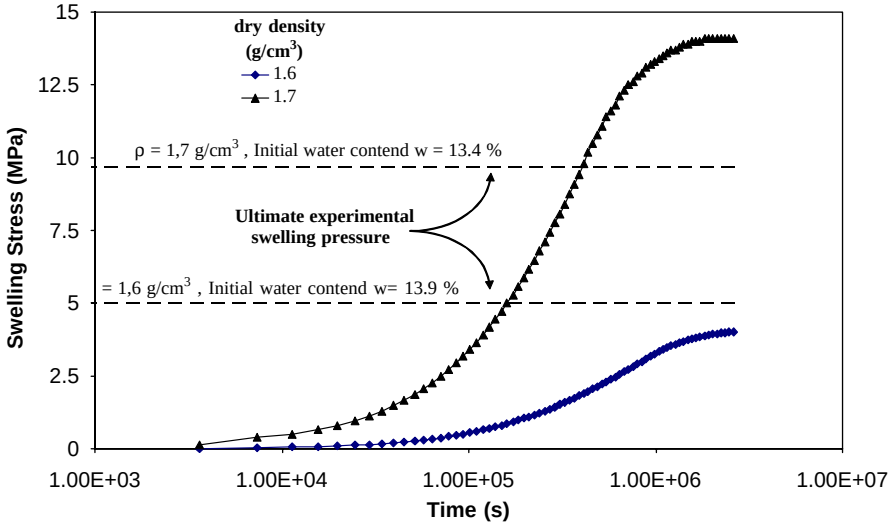

Fig. 5. Comparison of model prediction to experimental results of swelling pressure tests.

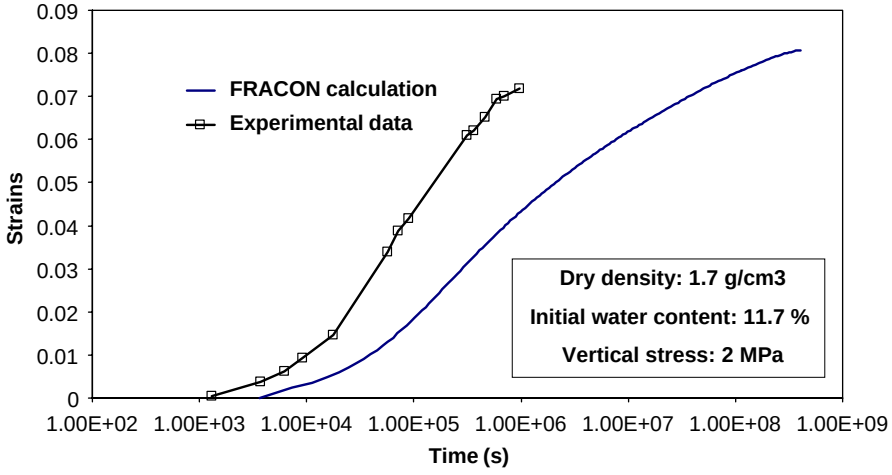

Fig. 6. Comparison of model prediction to experimental results of swelling tests under constant applied vertical stress.

sample being tested might be slightly different from the ones used in the FRACON code as detailed in Section 5.

6. Prediction of the bentonite response in the FEBEX in-situ experiment

The FEBEX gallery is circular in cross section, with diameter 2.28 m and length 70.4 m. It was excavated at a depth of approximately 450 m, in granitic rock. Two electrically powered heaters, with nominal diameter 0.9 m and length 4.54 m, were emplaced at the end of the gallery. Blocks of compacted bentonite were emplaced around the heaters to form a 17.4 m test section, isolated from the rest of the gallery by a concrete plug (Fig. 7).

The bentonite and heaters were installed between July 1, 1996 and October 15, 1996. Heating commenced on February 27, 1997 (set at time = 0), in the following three stages:

(i) Constant power output of 1200 W per heater for 20 days.
(ii) Constant power output of 2000 W per heater for the next 33 days.
(iii) Constant temperature control (between 95 and 100 °C) on the surface of the heaters from day 53.

The research teams participating in the DECOVALEX project were requested to predict temperature, relative humidity and stresses at selected locations and at times in the bentonite after the commencement of the heating (from day 0).

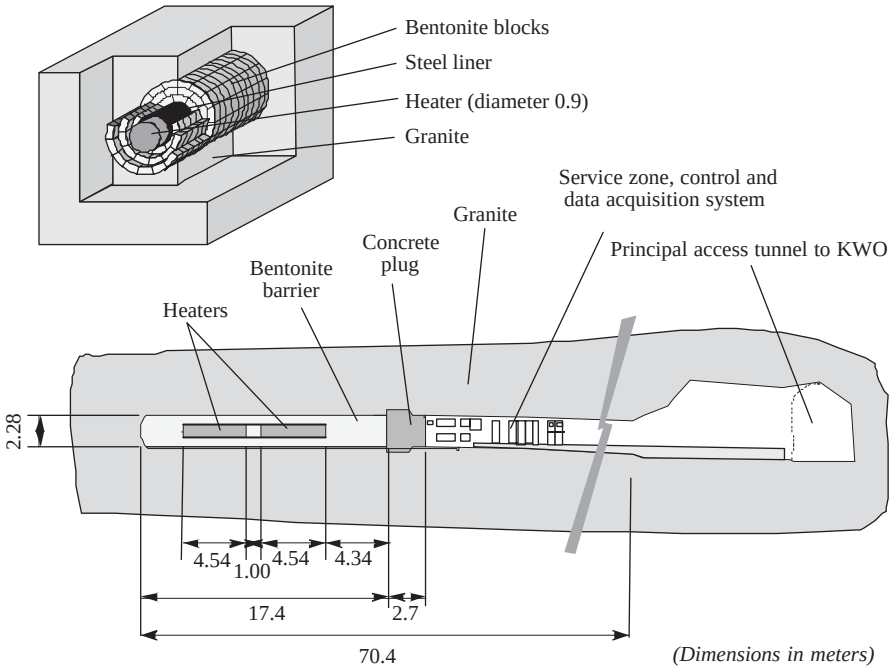

Fig. 7. Layout of the FEBEX in-situ heater experiment.

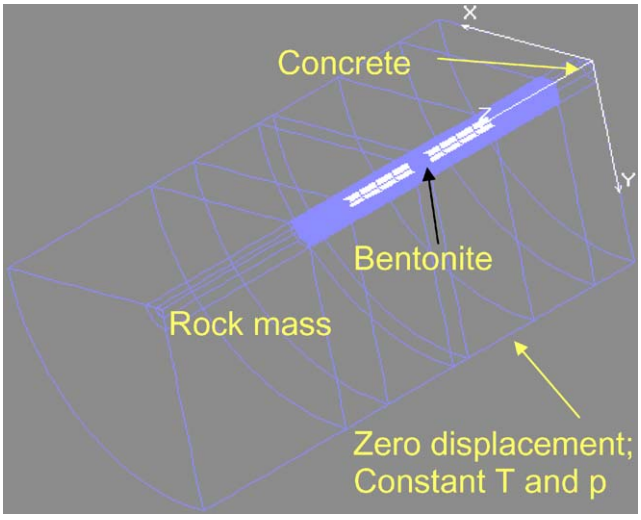

Fig. 8. Conceptual representation of the FEBEX heater experiment.

6.1. General modelling approach

Based on a review of the information [20,24] provided by the UPC and the authors' experience with similar type of in-situ experiments [1–5] the general following approach was adopted.

6.1.1. Conceptualisation

The conceptual model is schematically represented in Fig. 8. We assume radial symmetry around the axis of the FEBEX tunnel, with a radius of influence of approximately 11 m from the centreline of the tunnel. The FEBEX gallery is intersected by several structural features, such as fracture zones and lamprophyres zones, which are more hydraulically conductive than the relatively intact rock mass. However, in this paper, the above features were ignored and an equivalent homogeneous porous medium approach was adopted for the modelling of the rock mass. The above assumption originates from past experience gained from observations made at the Kamaishi Mine in Japan [1–5] where it was found that the THM behaviour of the bentonite was not influenced by the presence of discrete fractures in the rock mass but rather by the contrast in the permeability of the bentonite, and the bulk permeability of the rock mass. In our attempt to predict the response of the rock mass [25], these structural features had to be included.

6.1.2. Sequence of transient analysis using the FRACON code

In modelling the response of the bentonite, we computationally simulate as closely as possible, the actual test sequence. Each of the following phases were modelled with the FRACON code, with the results of the last time step of each phase being used as starting conditions for the subsequent phase:

(i) $t = -180$ day to $t = 0$: the emplaced bentonite was allowed to re-saturate isothermally.
(ii) $t = 0$ to 20 days: the heaters were set at an output of 1200 W each.

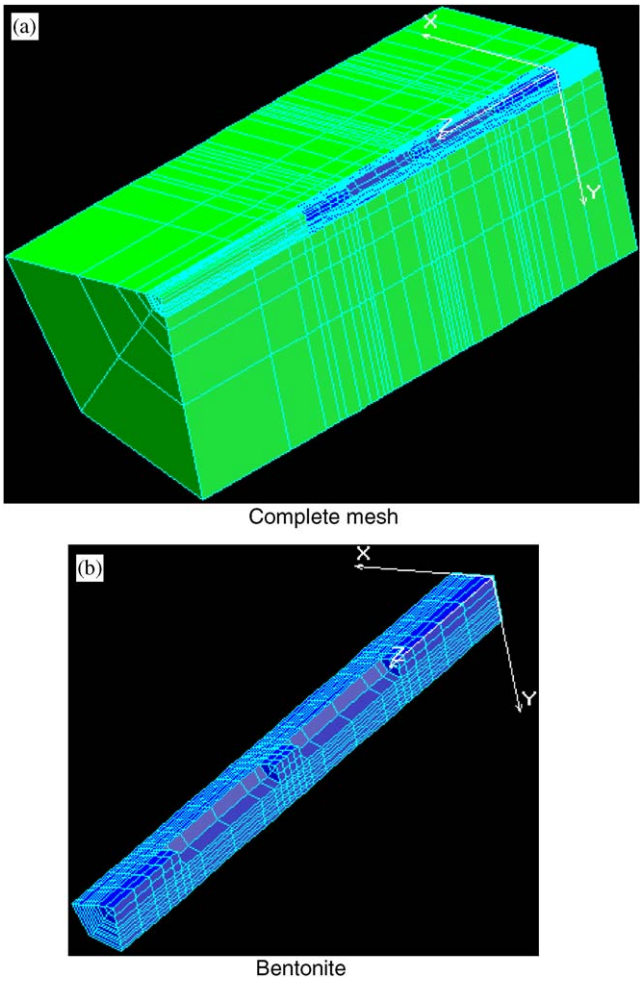

Fig. 9. Finite element mesh for the modelling of the FEBEX T-H-M experiment.

(iii) $t = 20$ to 53 days: the heaters were set at an output of 2000 W each.
(iv) $t = 53$ to 450 days: the surface of the heaters was set at 100 °C.

6.2. Finite element discretization

The finite element mesh for the simulation of the THM problem using the FRACON code is shown in Fig. 9; it comprises 876 isoparametric elements and 5093 nodes. It should be noted that the model is axisymmetric. However, since in its current version the FRACON code has only three-dimensional elements, a 3D representation is adopted.

Three material types are represented in the finite element model:

(i) The bentonite with constitutive equations and properties as previously described.
(ii) The rock mass which is assumed to be homogeneous and linear elastic, as justified in Section 1. The following values of the elastic constants and the permeability were based on our previous modelling of the excavation of the FEBEX gallery [26]: $E = 10\,\text{GPa}$, $v = 0.37$, $k_{\text{radial}} = 5 \times 10^{-19}\,\text{m}^2$; $k_{\text{axial}} = 5 \times 10^{-18}\,\text{m}^2$.
(iii) The concrete which is also assumed to be homogeneous, isotropic and linear elastic, with the following assumed properties: $E = 30\,\text{GPa}$, $v = 0.2$, $k = 10^{-21}\,\text{m}^2$.

The outside boundaries of the rock mass are assumed to be fixed against normal displacement, and are specified to remain at a constant temperature (12 °C). The measured steady state pressure in the rock in the vicinity of the gallery varies between 0 (atmospheric) and less than 1 MPa. These values are very small to influence the hydraulic response of the bentonite. For the sake of simplicity, we have assumed that the outside boundary of the rock mass is maintained at a constant pressure of 0 MPa. The heaters are not explicitly modelled; instead, the boundaries between the heaters and the bentonite are assumed to be fixed at zero normal displacement and zero fluid flux (very rigid and impermeable heaters), and an imposed power output is specified at either a constant rate or constant temperature depending on the sequence of heating. The initial conditions (at time $= -180$ days) are $T = 12\,^{\circ}\text{C}$ throughout the model, $p = 0$ in the rock and concrete, and initial water content of 13.4%.

6.3. Comparison of predicted and measured results

We now present the results for different T-H-M output parameters at points and along sections where these parameters were experimentally measured. It should be noted again that the model was used to perform "blind predictions", i.e. the measured values were provided to the research teams only a posteriori.

6.3.1. Relative humidity

The relative humidity H_r is a function of suction and temperature as given in the Kelvin's equation:

$$H_r = \text{Exp}(-sm_v v_w / R/(T + 273.16)), \quad (39)$$

where m_v is the specific volume of water ($0.001\,\text{m}^3/\text{kg}$), v_w is the molecular mass of water vapour (18.016×10^{-3} kg/mol) and R is the universal gas constant (8.31432 J/(mol K)).

The evolution of relative humidity at three points E1H, E1C, E1G, is shown in Fig. 10. As expected, the results show that resaturation is faster near the rock (E1G). Near the heater (point E1H) the drying effects persist up to and probably well beyond 1000 days. At point E1C, midway between the heater and the rock, the relative humidity increases in the early stages up to approximately 15–20 days, most likely as a result of

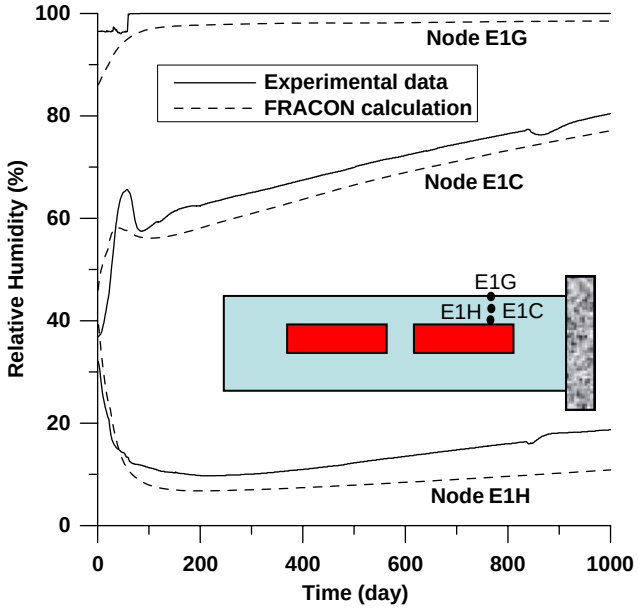

Fig. 10. Evolution of relative humidity.

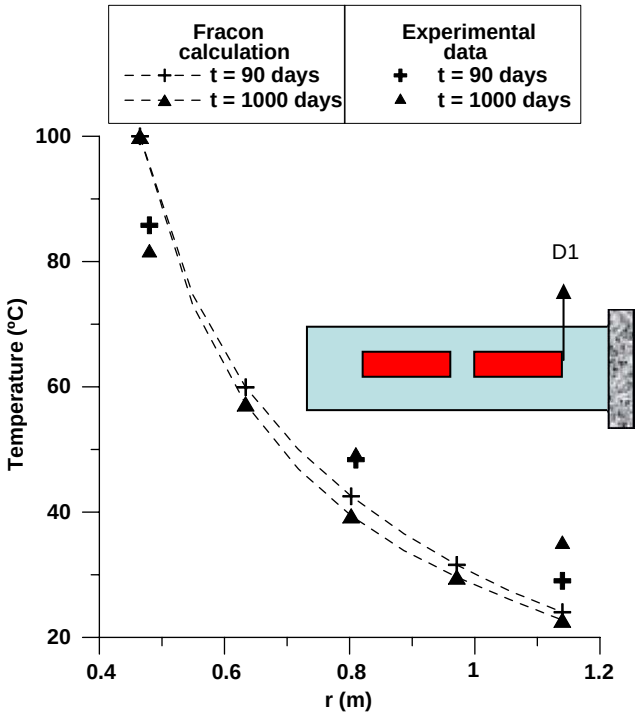

Fig. 11. Distribution of temperature along radial direction D1.

vapour condensation. After this time, the relative humidity decreases when the thermal pulse reaches the point E1C, until approximately 100 days, when it increases again, due to water input from the rock mass. Fig. 10 also shows excellent agreement between the predicted and experimental results for the evolution of the relative humidity. It should also be noted in Fig. 10,

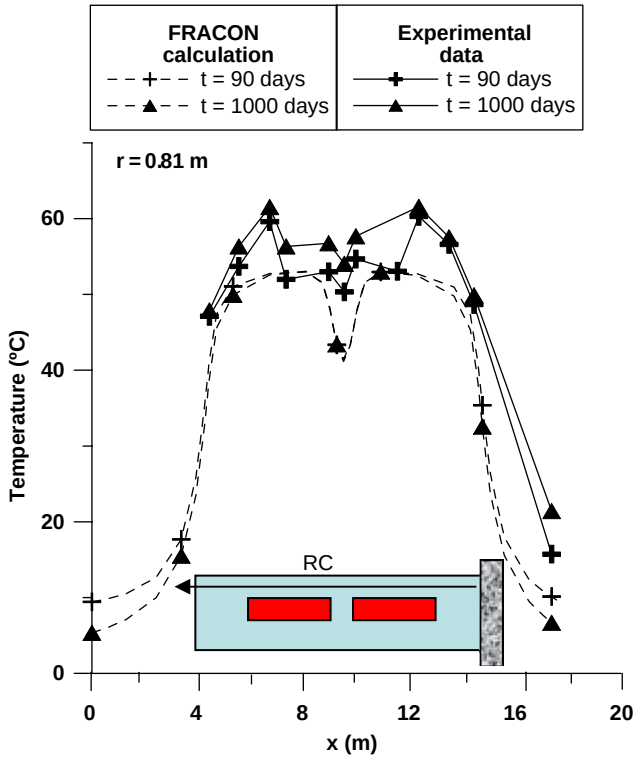

Fig. 12. Temperature distribution along axial direction RC1.

that at $t = 0$, the relative humidity is not the same for all points. This comes from the fact that time zero corrresponds to the time when heating is started. Before time zero, there is a period of isothermal resaturation as explained in Section 6.1.3 (corresponding to phase i).

6.3.2. Temperature

The distributions of temperature along one radial section and one axial section are shown in Figs. 11 and 12, respectively. It could be seen, from both the predicted and measured values, that a steady state thermal regime is attained not too much later than 90 days. The model generally underpredicts the values of temperature, due to the constant temperature conditions of 12 °C imposed on the outer boundaries of the finite element model. The predictions could be improved if these boundaries were defined at larger distances.

6.3.3. Stresses

The evolution of total radial stress at points E2G1, E2G2 (near the rock interface) and E2H1 (near the heater 2) are shown in Fig. 13. Compressive stress values of up to 1.4 MPa were calculated at the rock interface (E2G2). Near the heater the stresses are predicted to be small, attaining a maximal value of 0.1 MPa and originating from thermal expansion of the bentonite. The model predicts that a steady state stress regime is attained very rapidly in the bentonite, due to swelling of

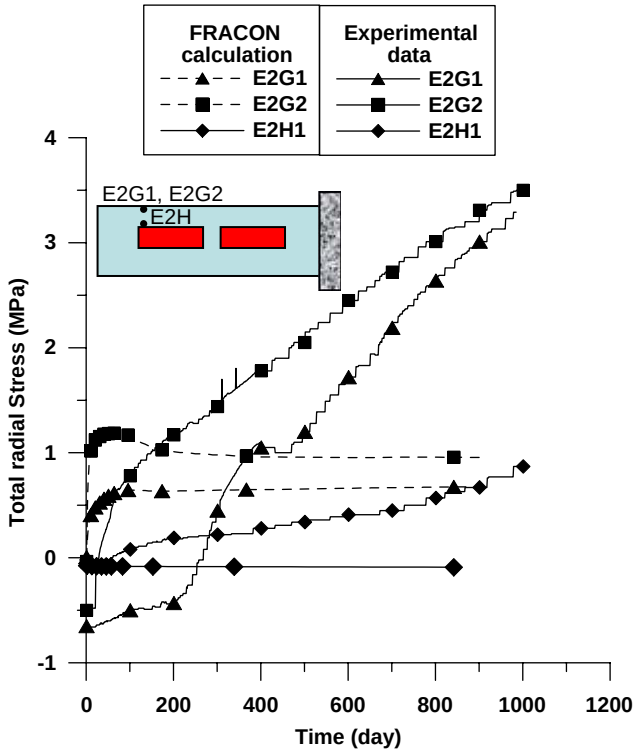

Fig. 13. Evolution of radial stresses in bentonite.

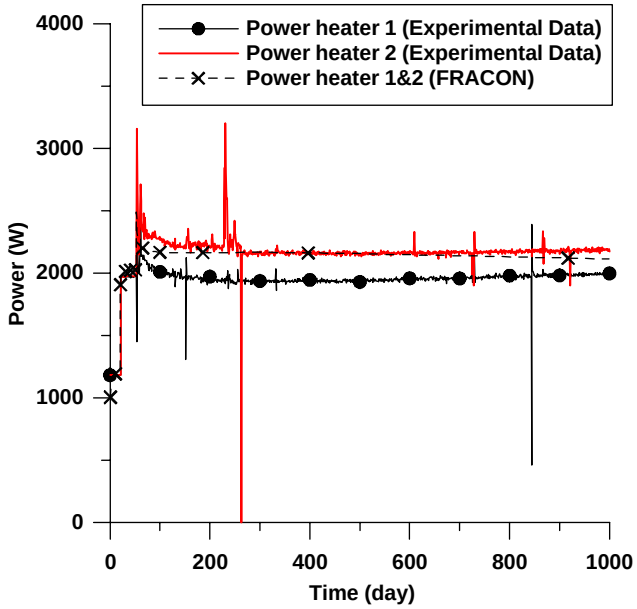

Fig. 14. Power output from heater.

the bentonite from resaturation. The measured values however show that the stress is still increasing at 1000 days. We believe that heating of the surrounding rock mass results in thermal expansion of the porewater and the solid matrix. Since the coefficient of thermal expansion of the water is higher than that for the solid matrix, this results in an increase in the porewater pressure. This water pressure increase was in fact predicted in our simulation of the rock mass response [25] and would be transmitted to the total stress measured in the bentonite. That phenomenon is, however, neglected in the present model since we impose a zero pore pressure in the rock mass.

6.3.4. Heater output

The power output from the heaters is shown in Fig. 14. The output is predicted to be almost the same for the two heaters. During the temperature control phase, the power would have to be increased initially to raise the temperature at the surface of the heaters to the pre-set value of 100 °C; this power will then decrease to an asymptotic value. The power output predicted by the model agrees very well with the measured value, although the measured output from heater 2 (near the concrete block) is higher than that from heater 1.

7. Conclusions

The FEBEX T-H-M experiment performed at the Grimsel site, Switzerland, is a valuable and important project which should lead to an improvement in the understanding of the behaviour of the bentonite barrier around heat-emitting nuclear fuel waste (NFW) containers. Such large-scale field experiments should always be undertaken with the simultaneous development of constitutive and computational models to interpret the experiments. In our contribution to this work, we have followed the process of model development and calibration with laboratory experiments prior to using the developed computational model to perform prediction of the response of the in-situ experiment. The FEBEX bentonite possesses strong nonlinear behaviour in the unsaturated state. In order to simulate such behaviour, we have adopted an incrementally nonlinear poro-elasticity approach. In this approach, the coefficients of the poroelastic equations are assumed to be functions of suction and the void ratio, and summarized by the state-surface equation which has been derived from suction-controlled oedometric tests performed by the Spanish research organizations UPC and CIEMAT.

The equations of poro-elasticity were solved with the finite element code FRACON. The FRACON code was used first to predict the bentonite response in laboratory H-M experiments. The swelling behaviour upon resaturation of the bentonite under both constrained and free swelling conditions were adequately predicted by the model. The model was then used to predict the bentonite response in the in-situ T-H-M experiment at the FEBEX gallery. The FRACON code correctly predicted that the bentonite would resaturate from the rock interface. Near the heater, it also correctly

predicted that initial drying will take place, followed by a slow resaturation. The model predicted that at the end of 1000 days of heating, resaturation of the bentonite was still incomplete, a fact that is confirmed by experimental data. The model predicted thermal behaviours in the bentonite which are also consistent with the experimental results. For example, the power output predicted from the model agrees well with the measured output and, comparably to the experimental data, the temperature distribution was predicted to reach a steady state regime in over 90 days. However, the absolute values of temperature were under-predicted, due to artificial boundary conditions imposed on the finite element mesh. Due to re-saturation, the bentonite has a tendency to swell. Since this swelling is impeded by the surrounding rock, a compressive radial stress of the order of 1.5 MPa is predicted near the rock interface. The measured values of radial stress show values higher than the predicted values. We believe that thermally induced pore pressure increase in the surrounding rock mass is an additional component contributing to increases in stress. That component was neglected in our computations.

Acknowledgements

The authors sincerely thank the Canadian Nuclear Safety Commission (CNSC) for its financial support; ENRESA for providing experimental data from the FEBEX project; and colleagues in the DECOVALEX International cooperative project and the CNSC for fruitful cooperation, discussion and peer review of our work. The opinions expressed in this paper are those of the authors' and do not necessarily reflect the opinions of the either the CNSC or McGill University.

References

[1] Borgesson L, Chijimatsu M, Fujita T, Nguyen TS, Rutqvist J, Jing L. Thermo-hydro-mechanical characterisation of a bentonite-based buffer material by laboratory tests and numerical back analyses. Int J Rock Mech Min Sci 2001;38(1):95–104.

[2] Chijimatsu M, Fujita T, Sugita Y, Amemiya K, Kobayashi A. Field experiment, results and THM behavior in the Kamaishi mine experiment. Int J Rock Mech Min Sci 2001;38(1):67–78.

[3] Nguyen TS, Borgesson L, Chijimatsu M, Rutqvist J, Fujita T, Hernelind J, Kobayashi A, Onishi Y, Tanaka M, Jing L. Hydro-mechanical response of a fractured granitic rock mass to excavation of a test pit- the Kamaishi mine experiment in Japan. Int J Rock Mech Min Sci 2001;38(1):79–94.

[4] Rutqvist L, Borgesson L, Chijimatsu M, Kobayashi A, Jing L, Nguyen TS, Noorishad J, Tsang C-F. Thermohydromechanics of partially saturated geological media: governing equations and formulation of four finite element models. Int J Rock Mech Min Sci 2001;38(1):105–28.

[5] Rutqvist L, Borgesson L, Chijimatsu M, Jing L, Nguyen TS, Noorishad J, Tsang C-F. Coupled thermo-hydro-mechanical analysis of a heater test in fractured rock and bentonite at Kamaishi mine—comparison of field results to predictions of four finite element codes. Int J Rock Mech Min Sci 2001;38(1):129–42.

[6] EURATOM. Full-scale engineered barriers experiment for a deep geological repository for high-level radioactive waste in crystalline host rock (FEBEX project). Report EUR 19147, Directorate-General for Research, European Commission, rue de la Loi/Wetstraat 200, B-1049 Brussels, 2000.

[7] Olivella S, Carrera J, Gens A, Alonso EE. Nonisothermal multiphase flow of brine and gas through saline media. Transp Porous Media 1994;15:271–93.

[8] Thomas HR, He Y, Sansom MR, Li CLW. On the development of the thermo-mechanical-hydraulic behaviour of unsaturated soils. Eng Geology 1996;41:197–218.

[9] Thomas HR, He Y, Onofrei C. An examination of the validation of a model of the hydro/thermo/mechanical behaviour of engineered clay barriers. Int J Num Anal Meth Geomech 1998;22:49–71.

[10] Gens A, Garcia-Molina AJ, Olivella S, Alonso EE, Huertas F. Analysis of a full scale in situ test simulating repository conditions. Int J Num Anal Meth Geomech 1998;22:515–48.

[11] Matyas EL, Radhakrishna HS. Volume change characteristics of partially saturated soils. Geotechnique 1968;30(4):432–48.

[12] Fredlund DG, Morgenstern NR. Stress state variables for unsaturated soils. J Geotech Eng Div ASCE 1977;103:447–66.

[13] Alonso EE, Gens A, Josa A. A constitutive model for partially saturated soils. Geotechnique 1990;40:405–30.

[14] Olivella S, Gens A. Vapour transport in low permeability unsaturated soil with capillary effects. Transp Porous Media 2000;40:219–41.

[15] Bishop AW, Blight GE. Some aspects of effective stress in saturated and partially saturated soils. Geotechnique 13: 177–97.

[16] Biot MA. General theory of three dimensional consolidation. J Appl Phys 1941;12:15–164.

[17] Fredlund D, Rahardjo H. Soil mechanics for unsaturated soils. New York: Wiley; 1993.

[18] Nguyen TS, Selvadurai APS. Coupled thermal-hydrological-mechanical processes in sparsely fractured rock. Int J Rock Mech Min Sci 1995;32:465–80.

[19] Lloret A, Alonso EE. State surfaces for partially saturated soils. Proceedings of the International Conference on Soils Mechanics and Foundation Engineering, vol. 2. Balkema, 1995. p. 557–62.

[20] ENRESA. FEBEX full-scale engineered barriers experiment in crystalline host rock- Bentonite: origin, properties and fabrication of blocks. Publicacion Tecnica 05/98. ENRESA. Emilio Vargas, 7-28043, Madrid, 1998.

[21] Bear J. Dynamics of fluids in porous media. Amsterdam: Elsevier; 1972.

[22] Bishop AW. The influence of an undrained change in stress on the pore pressure in porous media of low compressibility. Geotechnique 1973; 435–42.

[23] de Marsily G. Quantitative hydrogeology, appendix 2. New York: Academic Press Inc.; 1986.

[24] UPC. Task definition: DECOVALEX III, Task 1: Modelling of FEBEX in-situ test, Part B: Thermo-hydro-mechanical analysis of the bentonite behaviour. Polytechnical University of Catalonia, Barcelona, Spain, 2000.

[25] Selvadurai APS, Nguyen TS, Armand G. Computational predictions of the rock mass response in an in-situ heater test at the Grimsel site. Canadian Geotechnical Conference, Winnipeg, 2003.